VIABILITY GRADIENTS IN BIOFILM: A SLIPPERY SLOPE?

(Viability Gradients)

CK Hope

Unit of Plaque Related Diseases, School of Dental Sciences, University of Liverpool. L69 3GN. U.K.

Abstract

Are the fluorescence profiles observed in biofilm an artefact of confocal microscopy and sample topography? A mathematical model has been constructed that replicates these profiles in a homogenous 'biofilm'. However; direct measurement of metabolic activity in biofilm shows that viability profiles do exist and are therefore structural motifs worthy of study.

Keywords

Cell viability, fluorescence, biofilm, confocal laser scanning microscopy

Biofilms of bacteria are not homogeneous structures and contain many nonviable cells. These phenomena are due in part to the development of physicochemical gradients within the biofilm, which in turn are manifested as gradients of cell viability. Confocal laser scanning microscopy (CLSM) used in conjunction with fluorescent indicators of cell membrane integrity is a powerful technique for measuring viability gradients within biofilm. However; is it possible that the observations are themselves merely an artefact of confocal microscopy?

The confocal scanning microscope was invented in 1955 as a step towards 'the perfect microscope', one that would be able to examine each point in a specimen and measure the amount of light scattered or absorbed by that individual point (Minsky 1988). It was effectively two microscopes bolted together, one to illuminate a point in the sample with an intense spot of light and another to observe this. The foci of these two microscopes were the same; hence they were termed 'confocal'. This equipment was developed in the days before lasers, so intense arc illumination sources were used. Although carbon arcs were the brightest available they were unreliable so zirconium arcs, the second brightest, were used instead. Whilst the optical principles of this device worked well, it was extremely difficult to analyse or visualise the data generated. This changed in the 1980's upon the advent of affordable, reliable computer systems capable of undertaking image analysis and data storage. Modern CLSM uses a focussed spot (or multiple spots or a slit) of laser light to scan across the sample whilst a pinhole aperture blocks aberrant light from areas outside of the focal plane of interest. CLSM has been used for almost two decades to undertake the optical sectioning of microbial biofilms to produce three-dimensional data sets (Lawrence *et al.* 1991).

Fluorescent dyes (fluorophores) are now a fundamental component of CLSM. Fluorescence is the molecular adsorption of a photon which in turn triggers the emission of another photon of a longer wavelength (due to the Stokes shift); the remaining energy is lost as molecular vibration or shed as heat. Put simply, a fluorescent material adsorbs light of one colour and emits another.

This phenomenon allows one to illuminate a specific fluorophore with light of one wavelength and selectively collect the resulting emissions using filters to obstruct light of unwanted wavelengths, whilst the confocal optics block light from unwanted focal planes.

CLSM analysis of biological samples typically uses fluorophores that are associated with specific matrix / biofilm components. In the case of microbial biofilm these fluorophores / targets could included:

1. Calcofluor white: Binds to β-linked polysaccharides (i.e. to label extracellular polysaccharide).
2. Fluorescent *in situ* hybridisation (FISH): Detect the presence (or absence) of specific 16s rRNA sequence in multispecies biofilm (i.e. for the identification of microbial species).
3. Fluorescent indicators of membrane integrity (i.e. to reveal cell viability).
4. Green Fluorescent Protein integrated into the genome (i.e. used as a reporter of gene expression / metabolic activity / biosensor).

The molecular Probes™ LIVE/DEAD stain system detects nonviable bacteria by a red fluorescent dye (DEAD - propidium iodide) which is membrane impermeant and as such is excluded from entering intact, healthy cells. Viable bacteria are detected by a complimentary, green fluorescent dye (LIVE – SYTO9™) which is membrane permeable and stains all cells. When these dyes intercalate DNA their fluorescence increases significantly, therefore; unbound dyes in the *milieu extérieur* do not interfere with the detection of the stains within bacterial cells. If both dyes are present in a cell (i.e. a bacterium

with a damaged membrane), the DEAD stain displaces the LIVE stain from the nucleic acid due to its much higher affinity to intercalate DNA – such a cell will fluoresce red (DEAD).

CLSM data can be studied by a variety of image analysis techniques to yield numerical data regarding biofilm architecture (Wood *et al.* 2000), metabolic activity (Macfarlane and Macfarlane 2006), composition (Daims *et al.* 2006) and commensal interactions (Egland *et al.* 2004). Our previously published work regarding the spatial distribution of cell vitality in biofilm is based upon depth related trends observed using fluorescent indicators of membrane integrity. These data were gathered by CLSM and derived from plotting the total image fluorescence values against the depth of the optical section into the biofilm (Hope *et al.* 2002). To facilitate a degree of reproducibility between experiments, a biofilm tower (i.e. a high point) was centred in the confocal image stack (figure 1). The results typically produced a bell shaped curve of depth-related fluorescence distribution (figure 3). These data were then normalised (i.e. maximum image fluorescence = 1) and used to compare the distribution of viable and nonviable bacteria in biofilm (Hope and Wilson 2003a; Hope *et al.* 2002). Variations of this technique have also been applied by other groups and their findings have been similar to ours (Table 1) (Auschill *et al.* 2001; Arweiler *et al.* 2004; Netuschil *et al.* 1998; Pratten *et al.* 1998; Zaura-Arite *et al.* 2001; Hope *et al.* 2002; Hope and Wilson 2003b; Hope and Wilson 2006; Watson and Robinson 2005; Dalwai *et al.* 2006).

We were initially concerned that the viability profiles revealed by analysing image fluorescence could be an artefact caused by the inter-relationship of biofilm topology and the loss of image contrast which occurs with increasing depth in CLSM imaging. Since the biomass contained within an optical section (generally) increases with depth into the biofilm, this will correspond with an increase in fluorescence due to the presence of more fluorescent material. This effect will be apparent up to a depth of approximately 40 µm, being the point where the absorption of photons emitted by the fluorophore causes image fluorescence to decrease towards zero (Vroom *et al.* 1999).

A mathematical model was constructed to demonstrate this perceived phenomenon based upon an idealised hemi-spherical biofilm of radius 80 µm (figure 2). In this model, the amount of fluorescent material within the 'optical section' increases with depth into the hemi-sphere. Fluorescence is distributed homogenously within this hemi-spherical model. Quenching of emitted photons is modelled at a linear rate beyond 40 µm depth until total absorbance at the base of the biofilm where no fluorescence is detectable. The resulting 'fluorescence profile' through this *in silico* model (figure 3) is similar to those which have been previously reported *in actu* (figure 1) and the conformity between these two facets would no doubt be even closer if a more complicated shape and a non-linear co-efficient of adsorption were incorporated into the mathematical model.

The result of this mathematical model was initially thought to be the reason why the 'typical' viability profiles we had previously observed in supragingival

plaque biofilms were again evident in subgingival plaque – even though individual optical sections presented a nonviable outer layer of bacteria surrounding a viable interior (Hope and Wilson 2006). This contradiction in subgingival plaque biofilm was discussed and it was suggested that if the extent of nonviable bacteria in the outer layers was minimal, then although it might present itself to the observer as nonviable outer layer, it would not affect image analysis of depth related viability / fluorescence profiles.

It now seems as though our initial concerns have been allayed after the results published in a recent study (Beyenal *et al.* 2004). In these experiments, an optical microsensor was used to probe biofilms of *Staphylococcus aureus* which were engineered to express Yellow Fluorescent Protein. The microsensor measured fluorescence at different points within a biofilm microcolony (figure 4) and reported depth related profiles. They suggested that metabolic activity (vitality) increases with depth in the outer layers of the biofilm before decreasing in the deeper regions. The relative fluorescence profiles produced by the direct microsensor technique, which physically penetrated into the biofilm, were similar to those produced by CLSM. This suggests that viability profiles produced by CLSM are not an artefact of the process by which the images are captured (Table 1). It would be interesting to see if the fluorescence profiles through the *S. aureus* biofilms, as captured by CLSM, matched those produced by the microsensor.

Biofilm topography is without doubt an important consideration when using CLSM to capture transverse optical sections and subsequently measure the

spatial distribution of cell vitality in relation to depth. The reproducibility of this and similar techniques will be improved by taking steps to standardise which structural motifs of biofilm are analysed, along with more advanced 3-dimensional analysis (Hope and Wilson 2003b).

Acknowledgements

Thanks to Prof Zbigniew Lewandowski and Dr Haluk Beyenal for permitting the reproduction of the graph in figure 4. Thanks also to Dr John Smalley, University of Liverpool for editorial comments.

References

Arweiler, N.B., Hellwig, E., Sculean, A., Hein, N., and Auschill, T.M. (2004) Individual vitality pattern of in situ dental biofilms at different locations in the oral cavity. *Caries Research* **38**, 442-447.

Auschill, T.M., Arweiler, N.B., Netuschil, L., Brecx, M., Reich, E., Sculean, A., and Artweiler, N.B. (2001) Spatial distribution of vital and dead microorganisms in dental biofilms. *Archives of Oral Biology* **46**, 471-476.

Beyenal, H., Yakymyshyn, C., Hyungnak, J., Davis, C.C., and Lewandowski, Z. (2004) An optical microsensor to measure fluorescent light intensity in biofilms. *Journal of Microbiological Methods* **58**, 367-374.

Daims, H., Lucker, S., and Wagner, M. (2006) daime, a novel image analysis program for microbial ecology and biofilm research. *Environmental Microbiology* **8**, 200-213.

Dalwai, F., Spratt, D.A., and Pratten, J. (2006) Modeling shifts in microbial populations associated with health or disease. *Applied and Environmental Microbiology* **72**, 3678-3684.

Egland, P.G., Palmer, R.J., Jr., and Kolenbrander, P.E. (2004) Interspecies communication in Streptococcus gordonii-Veillonella atypica biofilms: signaling in flow conditions requires juxtaposition. *Proceedings of the National Academy of Sciences of the United States of America* **101**, 16917-16922.

Hope, C.K. and Wilson, M. (2003a) Cell vitality within oral biofilms. In *Biofilm Communities: Order from Chaos?* 269-284. Edited by A. McBain, D. Allison, M. Brading, A. Rickard, J. Verran and J. Walker. Cardiff: BioLine.

Hope, C.K., Clements, D., and Wilson, M. (2002) Determining the spatial distribution of viable and nonviable bacteria in hydrated microcosm dental plaques by viability profiling. *Journal of Applied Microbiology* **93**, 448-455.

Hope, C.K. and Wilson, M. (2003b) Measuring the thickness of an outer layer of viable bacteria in an oral biofilm by viability mapping. *Journal of Microbiological Methods* **54**, 403-410.

Hope, C.K. and Wilson, M. (2006) Biofilm structure and cell vitality in a laboratory model of subgingival plaque. *Journal of Microbiological Methods* **66**, 390-398.

Lawrence, J.R., Korber, D.R., Hoyle, B.D., Costerton, J.W., and Caldwell, D.E. (1991) Optical sectioning of microbial biofilms. *Journal of Bacteriology* **173**, 6558-6567.

Macfarlane, S. and Macfarlane, G.T. (2006) Composition and metabolic activities of bacterial biofilms colonizing food residues in the human gut. *Applied and Environmental Microbiology* **72**, 6204-6211.

Minsky, M. (1988) Memoir on Inventing the Confocal Scanning Microscope. *Scanning* **10**, 128-138.

Netuschil, L., Reich, E., Unteregger, G., Sculean, A., and Brecx, M. (1998) A pilot study of confocal laser scanning microscopy for the assessment of undisturbed dental plaque vitality and topography. *Archives of Oral Biology* **43**, 277-285.

Pratten, J., Barnett, P., and Wilson, M. (1998) Composition and susceptibility to chlorhexidine of multispecies biofilms of oral bacteria. *Applied and Environmental Microbiology* **64**, 3515-3519.

Vroom, J.M., De Grauw, K.J., Gerritsen, H.C., Bradshaw, D.J., Marsh, P.D., Watson, G.K., Birmingham, J.J., and Allison, C. (1999) Depth penetration and detection of pH gradients in biofilms by two-photon excitation microscopy. *Applied and Environmental Microbiology* **65**, 3502-3511.

Watson, P.S. and Robinson, C. (2005) The architecture and microbial composition of natural plaque biofilms. In *Biofilms: Persistence and Ubiquity*. 273-285. Edited by A. McBain, D. Allison, J. Pratten, D. Spratt, M. Upton, and J. Verran. Cardiff: BioLine.

Wood, S.R., Kirkham, J., Marsh, P.D., Shore, R.C., Nattress, B., and Robinson, C. (2000) Architecture of intact natural human plaque biofilms studied by confocal laser scanning microscopy. *Journal of Dental Research* **79**, 21-27.

Zaura-Arite, E., van Marle, J., and ten Cate, J.M. (2001) Confocal microscopy study of undisturbed and chlorhexidine-treated dental biofilm. *Journal of Dental Research* **80**, 1436-1440.

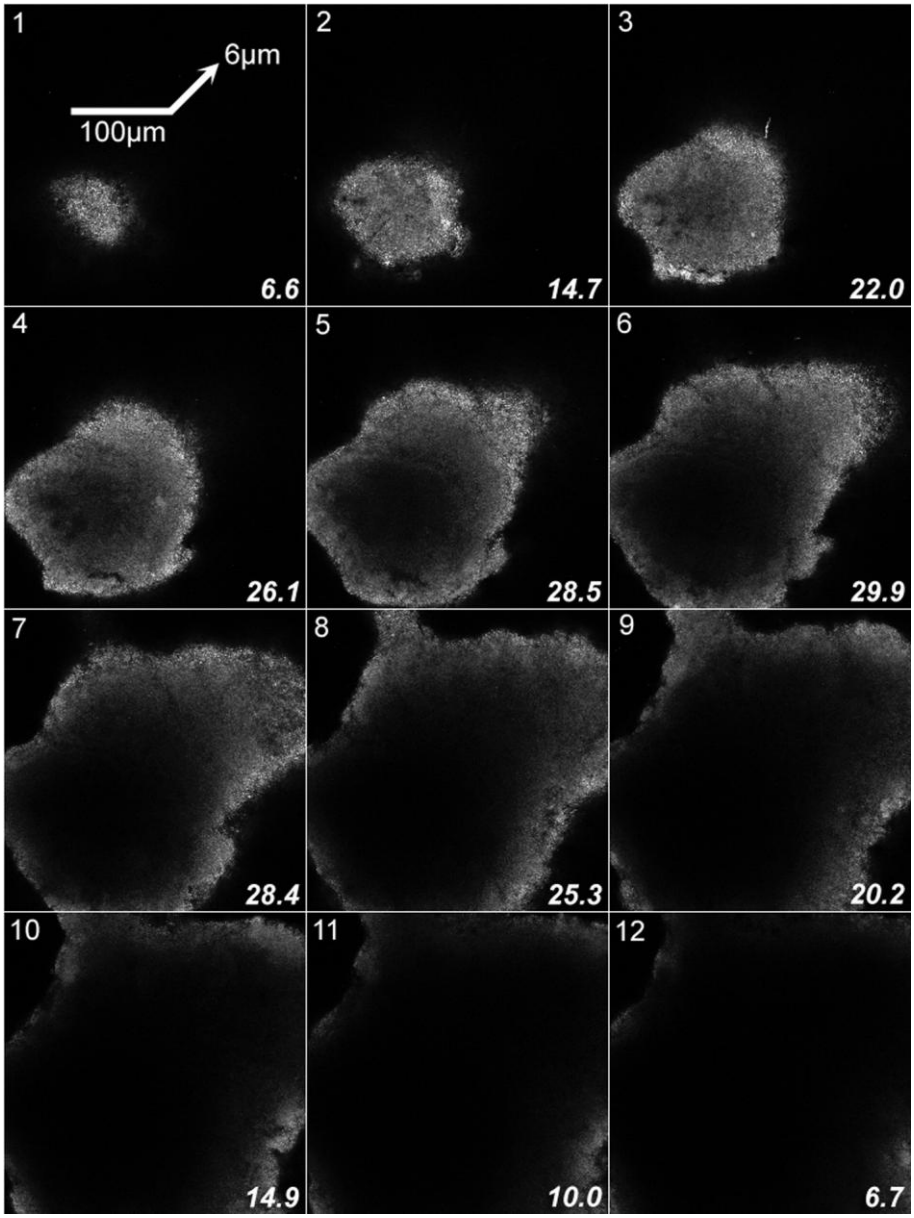

Figure 1 Sequence of twelve optical sections through subgingival oral biofilm stained with SYTO9 (300 x 300 x 72 µm; 6 µm slice separation). The average pixel brightness for individual images is given in the bottom right of each slice.

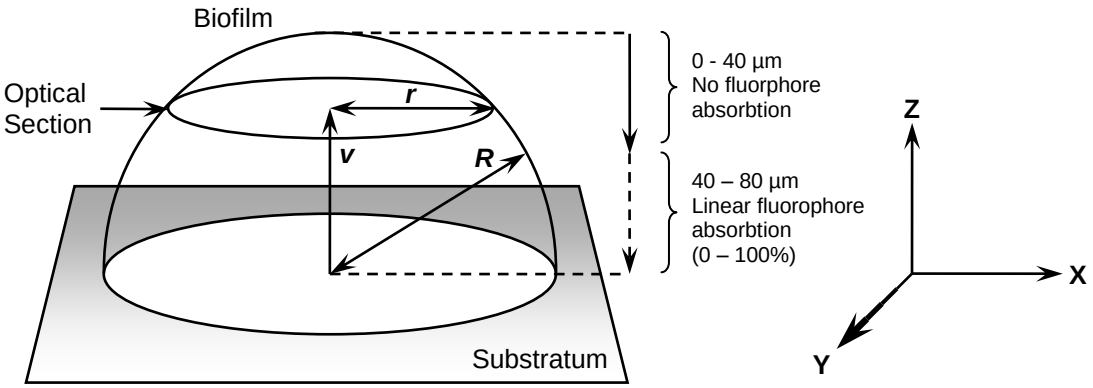

231

232 **Figure 2** Confocal image stack model based upon an idealised hemi-
233 spherical biofilm where; *R* is the radius of the sphere (80 µm), *v* is the height
234 of the optical section in the image stack and *r* is the radius of the circle formed
235 by the biofilm (at height *v*). In this model, the area (*a*) of a particular optical
236 section can be calculated using the equation, $a = \pi (R^2 - v^2)$ and is equal to
237 the image fluorescence. The fluorescence within the hemi-sphere is
238 distributed homogenously. The absorption of fluorophore photons by the
239 sample is modelled by a linear decrease in fluorescent intensity from 40 µm to
240 80 µm depth (0 to 100% adsorption).

241

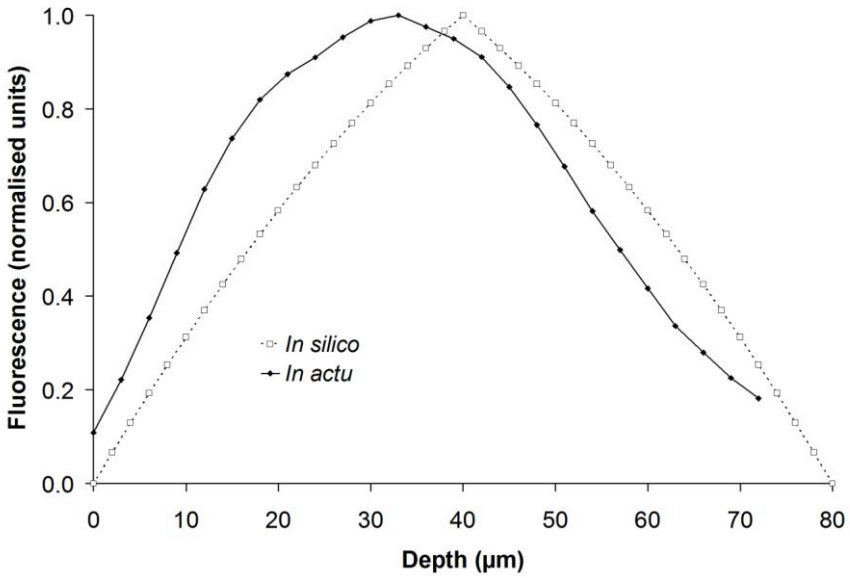

242

243 **Figure 3** Fluorescence profile through *in actu* subgingival plaque biofilm

244 grown in a CDFF (corresponding to figure 1) compared to a mathematical

245 model showing the fluorescence profile through an idealised biofilm *in silico*

246 (corresponding to figure 2).

247

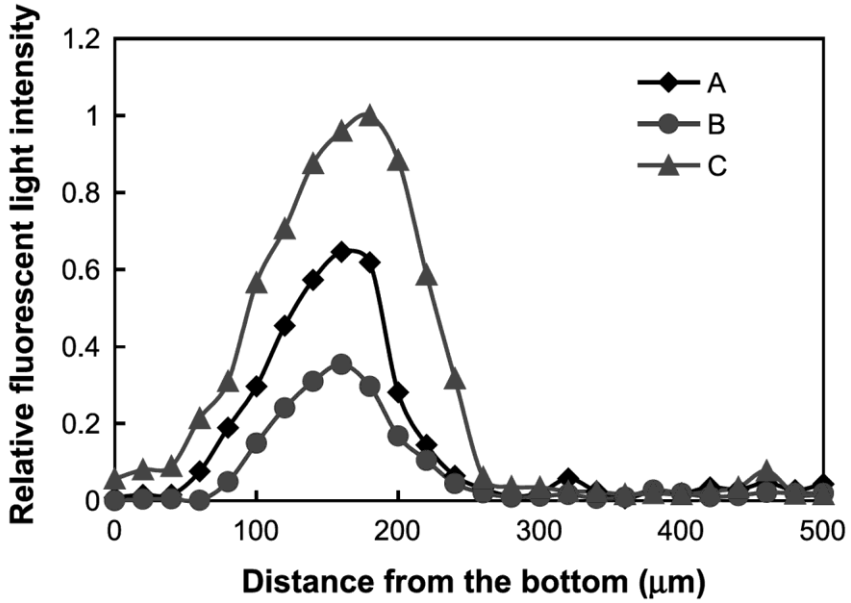

Figure 4 Relative fluorescence intensity profile measured in biofilm of *Staphylococcus aureus*. Plots A, B and C refer to different sites in a microcolony (Beyenal *et al.*, 2004).

253 **Table 1** Studies which comment upon on the spatial distribution of cell vitality
254 in oral biofilm. Asterisks (*) denote the common thread of cell vitality /
255 biomass distribution shown in figure 3.

Study	Principle	Findings
Arweiler 2004	CLSM. Vital staining; measured as percentage vitality in different optical sections.	1. Dead lower layers, live middle / upper layers, less live in outermost layers.* 2. Live lower layers, dead upper layers. 3. Thin disorganised layers.
Auschill 2001	CLSM. Vital staining; measured as percentage vitality in different optical sections.	Dead lower layers, live middle / upper layers, less live in outermost layers.*
Dalwai 2006	CLSM. Vital staining; viable and nonviable fluorescence measured in different optical sections.	Fluorescence distribution low in deep biofilm, higher in the middle layers, decreasing in the outermost layers.*
Hope 2002	CLSM. Vital staining; viable and nonviable compared by normalising fluorescence values in different optical sections.	Dead lower layers, live middle / upper layers, less live in outermost layers.*
Hope 2003	CLSM. Vital staining; analysis of data in 3-dimensions	Dead inner layers, live outer layers.*
Hope 2006	CLSM. Vital staining; viable and nonviable compared by normalising fluorescence values in different optical sections. Subgingival oral biofilm model.	1. Low fluorescence in lower layers, higher in middle / upper layers, lower in outermost layers.* 2. Horizontal sections suggested dead outer layers.
Netuschil 1998	CLSM. Vital staining; measured as percentage vitality.	Dead lower layers, live middle / upper layers, less live in outermost layers.*
Pratten 1998	CLSM vital staining.	Dead lower layers, live upper layers.*
Watson 2005	CLSM. Vital staining. Biomass recorded as total image fluorescence.	Low biomass in outer layers, increasing in middle layers, decreasing in deeper layers.*
Zaura-Arite 2001	CLSM. Vital staining. Comparison of percentage vitality at different depths.	No definitive pattern of vitality reported.

Other Related Studies

Study	Principle	Findings
Beyenal 2004	Direct measurement of Yellow Fluorescent Protein by an optical microsensor in *S. aureus*. (not oral biofilm, not CLSM)	Low fluorescence (metabolic activity) at biofilm surface, increasing with depth, decreasing in deeper layers.*
Egland 2004	CLSM. Distribution of specifically labelled bacteria (FISH) in a dual-species oral biofilm. (not vital staining)	Fluorescence distribution (biomass) low in deep biofilm, higher in the middle layers, decreasing in the outermost layers.*
Pratten 1998	Transmission electron microscopy. Comparison of cells from different depths in biofilm. (not CLSM)	Higher proportion of 'ghost' cells (assumed to be nonviable bacteria) in lower layers.*

256